Coordination Chemistry Reviews 254 (2010) 2546–2559

Contents lists available at ScienceDirect

Coordination Chemistry Reviews

journal homepage: www.elsevier.com/locate/ccr

Review

Expanded bite angles in tridentate ligands. Improving the photophysical properties in bistridentate Ru^{II} polypyridine complexes

Leif Hammarström, Olof Johansson*

Department of Photochemistry and Molecular Science, Uppsala University, BOX 523, S-751 20 Uppsala, Sweden

Contents

ARTICLE INFO

Article history:
Received 29 October 2009
Accepted 22 January 2010
Available online 1 February 2010

Keywords:
Ruthenium
Tridentate ligands
Polypyridine ligands
Luminescence
Photochemistry
Donor–acceptor

ABSTRACT

Bistridentate metal complexes as photosensitizers are ideal building blocks in the construction of rod-like isomer-free assemblies for intramolecular photoinduced charge separation. Approaches to obtain long-lived luminescent metal-to-ligand charge transfer excited states in bistridentate Ru^{II} polypyridine complexes via the manipulation of metal-centered state energies are discussed. Following an introduction to general strategies to prolong the excited state lifetimes, more recent work is explored in detail where tridentate ligands with expanded 2,2′:6′,2″-terpyridine cores are utilized. The synthesis of these tridentate ligands and their corresponding Ru^{II} complexes is covered. Bistridentate Ru^{II} complexes with microsecond metal-to-ligand charge transfer excited state lifetimes are described, and are used in electron donor–photosensitizer–electron acceptor assemblies for efficient vectorial photoinduced charge separation.

1. Introduction

Ruthenium(II) polypyridine complexes continue to be of much interest owing to their remarkable photophysical properties which are readily tuned by ligand modifications [1–5]. In combination with their facile synthesis, this class of complexes is an important target for artificial photosynthetic [3–5] and molecular electronic [6,7] applications. Trisbidentate complexes, *e.g.* $[Ru(bpy)_3]^{2+}$ (bpy is 2,2′-bipyridine) are typically used and display intense absorption in the UV and visible spectroscopic regions due to ligand-centered (LC) and metal-to-ligand charge transfer (MLCT) transitions, respectively. Excitation in any of the absorption bands leads to the rapid formation of a luminescent ^{3}MLCT excited state which decays to the ground state within ~1 μs [8]. In the presence of a quencher, energy transfer and/or electron transfer may compete with excited state decay. Such processes form the basis for the natural energy conversion schemes in photosystems I and II and are important to mimic in our strive to develop solar fuels based on sustainable resources.

Supramolecular approaches to artificial photosynthesis, where spatial control of the different components is achieved, has led to the development of multinuclear Ru^{II} polypyridine complexes as artificial antenna systems [5] and electron donor (D)–photosensitizer (P)–electron acceptor (A) complexes as charge

* Corresponding author.
E-mail address: olof.johansson@fotomol.uu.se (O. Johansson).

0010-8545/$ – see front matter © 2010 Elsevier B.V. All rights reserved.
doi:10.1016/j.ccr.2010.01.006

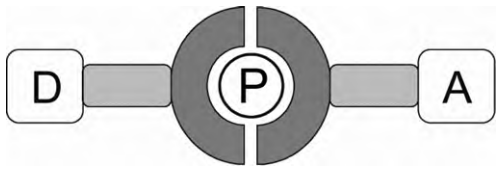

Fig. 1. Linear arrangement in a D–P–A triad based on a bistridentate Ru^{II} photosensitizer (*e.g.* $[Ru(tpy)_2]^{2+}$).

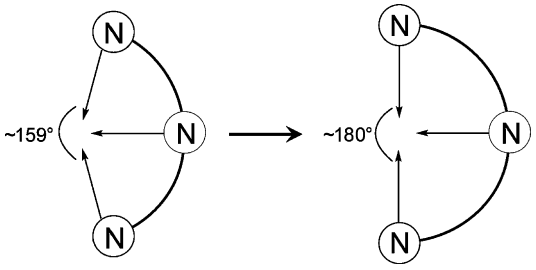

Fig. 2. The tpy ligands show unfavorable bite angles (159°, see for instance Ref. [80]) while tridentate ligands with an expanded tpy core may approach the ideal 180°.

separation devices [4,5,9–11]. As discussed thoroughly elsewhere [11,12], bistridentate Ru^{II} complexes (*e.g.* $[Ru(tpy)_2]^{2+}$, tpy is 2,2′:6′,2″-terpyridine) have structural advantages compared to the trisbidentate complexes. This is related to their achiral nature and higher symmetry (D_{2d} instead of D_3 for $[Ru(bpy)_3]^{2+}$) which is more favorable for the construction of linear arrays. Utilizing the C_2 axis running through the central pyridine 4′-positions, isomerically pure multicomponent systems have been prepared (Fig. 1) [10,11]. Although the ground state properties are similar to those for $[Ru(bpy)_3]^{2+}$, the excited state properties are poor. $[Ru(tpy)_2]^{2+}$ has a ^{3}MLCT excited state lifetime of only 250 ps [13], which often leads to inefficient electron/energy transfer to nearby quenchers [14–16]. This is due to unfavorable bite angles of the *mer* coordinated tpy ligands (Fig. 2) [17], and therefore a weak ligand field, leading to low-lying and thermally accessible metal-centered (^{3}MC) states. Population of antibonding e_g orbitals leads to strong distortion compared to the ground state and therefore rapid non-radiative decay and loss of energy.

Given the favorable structural properties of bistridentate complexes, major efforts have been focused on the design and synthesis of novel Ru^{II} complexes based on tridentate ligands where the photophysical properties are improved [18,19]. This article reviews approaches to achieve long-lived ^{3}MLCT excited states in bistridentate Ru^{II} complexes by directly affecting ^{3}MC states using tridentate ligands with expanded tpy cores (Fig. 2) [20]. A more octahedral coordination due to larger bite angles would ideally lead to a stronger ligand field and therefore a lower rate of population of the ^{3}MC state. A brief introduction to general strategies for achieving prolonged luminescent lifetimes in bistridentate Ru^{II} complexes is followed by recent progress on ligands with expanded tpy cores and the use of some of these complexes in charge separation assemblies.

2. Strategies to increase the ^{3}MLCT excited state lifetime in bistridentate Ru^{II} complexes

The ^{3}MLCT excited state lifetime of Ru^{II} polypyridine complexes is governed by radiative and non-radiative decay pathways to the ground state and the lifetime, τ, is given by Eq. (1). At room temperature, the excited state decay occurs to various extents by thermal population of ^{3}MC states ($k_{nr}^{act} = Ae^{-\Delta E/RT}$), while direct radiative (k_r) and non-radiative (k_{nr}) decays to the ground state (the latter governed by the energy gap law) dominate at lower temperatures. Two general strategies are conceivable to prolong the ^{3}MLCT excited state lifetime in bistridentate Ru^{II} complexes, both based on the notion that an increased energy gap (ΔE) between the ^{3}MLCT and ^{3}MC states will lead to a decrease in k_{nr}^{act}. The first strategy aims for a decrease of the ^{3}MLCT energy while the second strategy aims for an increase of the ^{3}MC energy (Fig. 3). For most Ru^{II} polypyridine complexes, ΔE reflects the activation barrier for irreversible surface crossing to the ^{3}MC state and not the difference in zero–zero energy [21]. In fact, recent DFT calculations for $[Ru(tpy)_2]^{2+}$ suggest that the ^{3}MC state is actually lower in energy than the ^{3}MLCT state [22].

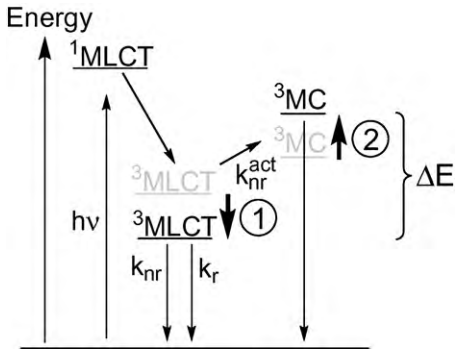

Fig. 3. Two strategies to increase the ^{3}MLCT excited state lifetime in bistridentate Ru^{II} complexes: (1) lower the ^{3}MLCT state, or (2) increase the ^{3}MC state. ΔE usually refers to the activation barrier.

$$\tau = \frac{1}{k_r + k_{nr} + Ae^{-\Delta E/RT}} \quad (1)$$

Much work has focused on the first approach, introducing substituents or other heterocycles that have a profound effect on the ^{3}MLCT energy. Although a lowering of the ^{3}MLCT excited state may be expected to increase k_{nr} according to the energy gap law, this can be balanced by an increase of the delocalization in the ^{3}MLCT excited state leading to a small displacement between the excited state and the ground state structures and therefore a smaller non-radiative (k_{nr}) rate-constant [23,24]. The second strategy, in contrast, has the advantage that the ^{3}MLCT excited state energy can, in theory, be left unaffected while the ^{3}MC state is selectively destabilized by a strong ligand field. A different approach to extend the luminescent lifetime is based on the introduction of additional organic chromophores with low-lying π–π^* triplet energy levels that repopulate the luminescent ^{3}MLCT excited state [25,26]. However, this decreases the population of the ^{3}MLCT state reflected in the fact that the emission and quantum yield of the ^{3}MLCT state is not increased and the strategy is therefore not a viable approach to increase the chemical reaction yield in multicomponent systems.

Maestri, Balzani, and Constable and co-workers introduced electron-accepting or electron-donating substituents in the 4′-positions of the tpy ligands to give Ru^{II} complexes where the ^{3}MLCT excited states are lower in energy than for $[Ru(tpy)_2]^{2+}$ (**1**–**4** in Fig. 4) [27,28]. With two electron-accepting substituents, one on each ligand, or complexes containing one electron-donating and one electron-accepting substituent, the complexes are luminescent at room temperature (τ = 1–50 ns) attributed to a decreased rate of population of ^{3}MC states. More recently, Hanan and Campagna and co-workers prepared cyano-functionalized Ru^{II} complexes and complex **5** luminesces at room temperature (τ = 75 ns) attributed to an increased energy gap between ^{3}MC and ^{3}MLCT states [29]. Ru^{II} complexes that provide increased delocalization in the ^{3}MLCT state leading to increased ^{3}MLCT–^{3}MC energy gaps (**6**–**10**) have also been much studied [30–34]. 4′-Alkynylene substituted complexes **7** [30] and **8** [33] prepared by Ziessel and Harriman and co-workers exhibit luminescent lifetimes of 50 ns and 44 ns, respectively, while the ^{3}MLCT excited state lifetimes in pyrimidine-substituted com-

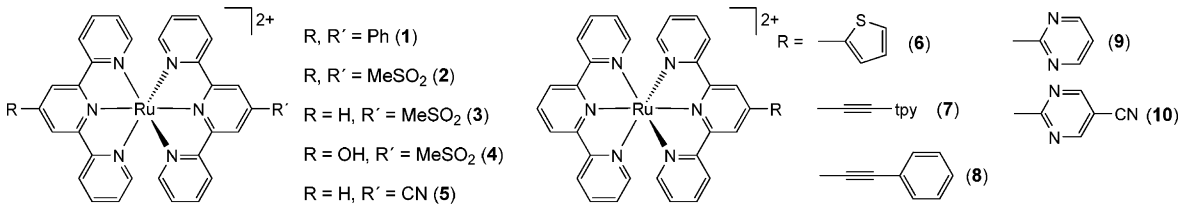

Fig. 4. Selected examples of mononuclear Ru^{II} complexes which exhibit prolonged ^{3}MLCT excited state lifetimes due to a lowering of the ^{3}MLCT state.

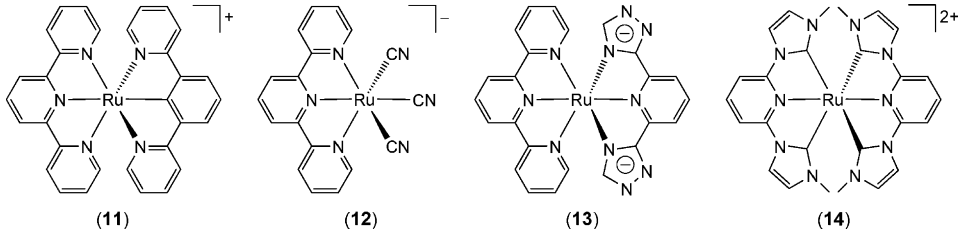

Fig. 5. Selected examples of Ru^{II} complexes with strong σ donors.

plexes **9** [31,34] and **10** [31,34] studied by Fang et al. are 8 ns and 200 ns, respectively. In **7**–**10**, increased delocalization on the acceptor ligand leads to reduced coupling between the ground state and the ^{3}MLCT state. The rate of non-radiative decay (k_{nr}) directly to the ground state is therefore lower than what would be expected solely on energy gap law arguments.

The second strategy to prolong the lifetime of the ^{3}MLCT excited state is to raise the energy of the ^{3}MC state using strong field ligands (Fig. 5). As such donors often also increase the energy of the metal-based t_{2g} orbitals while leaving the π^* orbitals of a second tridentate ligand unaffected, the strategy often leads to a concomitant decrease of the ^{3}MLCT state energy. Cyclometallating complexes where a nitrogen donor has been replaced with an anionic carbon, a strong σ donor, was an early approach introduced by Sauvage and co-workers and Constable and co-workers to generate luminescent bistridentate Ru^{II} complexes [35–37]. Both N^N^C and N^C^N ligands have been utilized where the latter (*e.g.* complex **11**) gave a luminescent Ru^{II} complex with τ = 4.5 ns [36]. As a result of the anionic donor, the ^{3}MLCT excited state energy is considerably decreased (λ_{max} = 784 nm) compared to N_6 analogues (Table 1), and the excited state decay in these complexes has been ascribed to a balance between activated decay via ^{3}MC states and non-radiative decay governed by the energy gap law [38]. Cyclometallated complexes are still of considerable interest [38,39] and have recently shown promise as photosensitizers for dye-sensitized solar cells [40]. Similar approaches using anionic donors were used by Scandola and co-workers in complex **12** (τ = 48 ns in DMSO) [41] and by Vos and co-workers in complex **13** (τ = 70 ns) [42,43], the former incorporating three strong field cyanide ligands which have replaced one tridentate ligand, and in the latter the substitution of two pyridine ligands to two triazole ligands. A somewhat different strategy was recently presented by Son et al. using carbene ligands

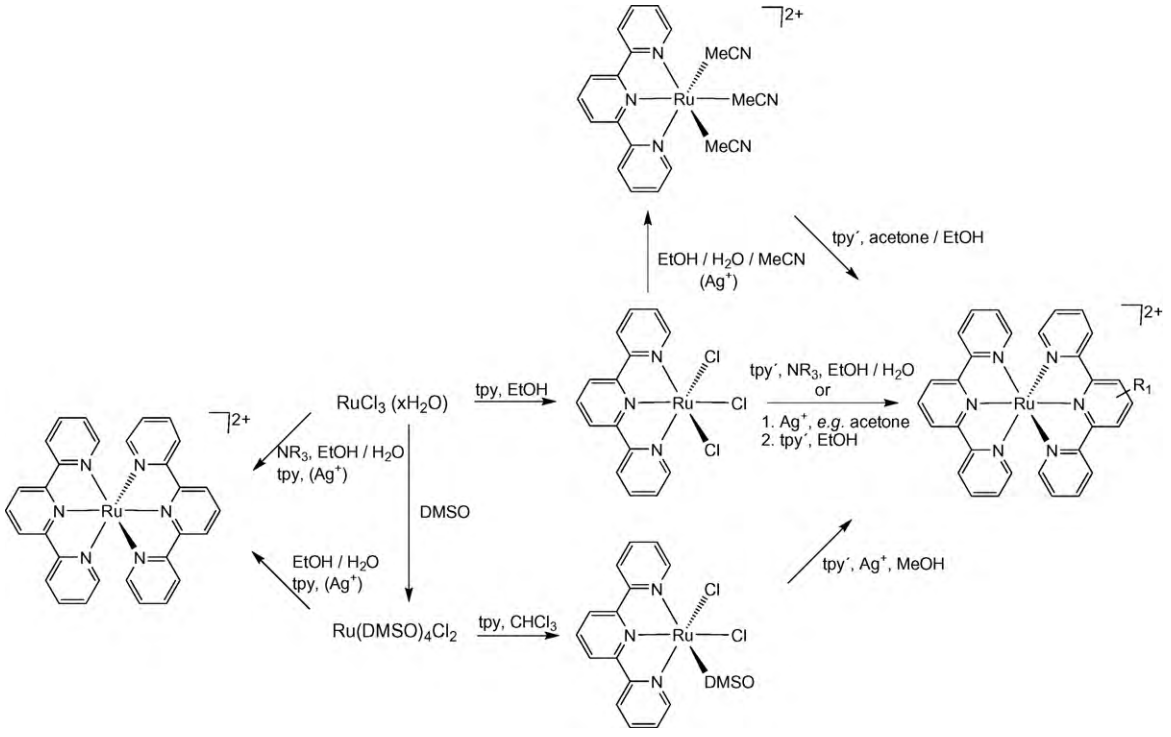

Scheme 1. Common synthetic protocols to tpy-based bistridentate Ru^{II} complexes.

(**14**) [44]. The absorption (and emission) is blue shifted compared to $[Ru(bpy)_3]^{2+}$ and the complex was reported to have a luminescent lifetime of 3.1 μs. Unexpectedly, the ^{3}MLCT excited state lifetime is longer in H_2O than in organic solvents which is not common for Ru^{II} polypyridine complexes.

Many of the approaches to prolong the ^{3}MLCT excited state lifetime use the 4′-positions on the central pyridines to introduce substituents to affect either the ^{3}MLCT and/or the ^{3}MC state. Although such an approach offers a convenient position for substitution, it also hinders the build up of linear multicomponent systems. A more attractive option, therefore, would be the realization of novel bistridentate Ru^{II} complexes where the positions that coincide with the principal axis (or comparable positions in low-symmetry complexes) remain unsubstituted, and where the ^{3}MLCT excited state energy is high. With this motivation, a new series of complexes were designed which incorporate tridentate ligands with an expanded tpy core and will be discussed after a general introduction to the synthesis of bistridentate Ru^{II} complexes.

3. Synthesis of bistridentate Ru^{II} complexes

The synthesis of bistridentate Ru^{II} polypyridine complexes usually relies on the preassembly of functionalized tpy ligands and subsequent reaction with an appropriate Ru source (Scheme 1), although a "chemistry on the complex" strategy has become popular. Homoleptic bisterpyridine Ru^{II} complexes can be conveniently obtained in a one-step reaction using either $RuCl_3{\cdot}xH_2O$ or $Ru(DMSO)_4Cl_2$ as precursor and two equivalents of the ligand in refluxing EtOH or EtOH/H_2O solutions. Alternatively, microwave-assisted heating in a high boiling solvent such as ethylene glycol often lead to high yields in short time. The reducing equivalent needed when using $RuCl_3{\cdot}xH_2O$ as precursor is provided by an added reductant, *e.g.* tertiary amines, or the alcohol solvent. The synthesis of heteroleptic complexes typically starts with the initial coordination of a tpy ligand to $RuCl_3{\cdot}xH_2O$ in an alcoholic solvent (EtOH) to give an insoluble $Ru(tpy)Cl_3$ species. In a subsequent step, a second tpy ligand is introduced under reducing conditions in refluxing EtOH or EtOH/H_2O solutions to give the heteroleptic complex usually in good yields (~50–90%). Prior to the reaction with the second tpy ligand, initial dechlorination using Ag^+ to form a Ru(tpy)-solvate species may facilitate coordination of the second ligand. The solvate intermediate is usually prepared *in situ*, but may also be isolated as has been done for $[Ru(tpy)(MeCN)_3]^{2+}$ [45]. For sensitive ligands an alternative stepwise method with *cis*-$Ru(tpy)(DMSO)Cl_2$ as intermediate was recently presented by Ziessel and co-workers who prepared heteroleptic complexes under mild conditions [46].

The stepwise synthesis of bistridentate complexes using $RuCl_3{\cdot}xH_2O$ relies on the different rates of coordination of the first and second tpy ligand. The attack of the second tpy ligand on the $Ru(tpy)Cl_3$ intermediate is believed to occur via the peripheral pyridine ligands at either a *cis* or *trans* position to the central pyridine ring of the coordinated tpy (Fig. 6) [47,48]. This leads to two distinct products, the desired $[Ru(N^N^N\text{-tpy})_2]^{2+}$ species (attack at the *cis* position) and a $[Ru(N^N^N\text{-tpy})(N^N\text{-tpy})Cl]^+$ byproduct (attack at the *trans* position). The latter complex is usually formed (if at all) in small amounts but has been isolated and are thermally stable but may be photochemically converted to the desired $[Ru(N^N^N\text{-tpy})_2]^{2+}$ complex [47].

4. Expanding the tpy core

4.1. 2,2′-Bipyridyl-pyridine ligands bridged by $-CR_2-$

The first approach to tridentate ligands with expanded tpy cores for Ru^{II} used 2,2′-bipyridyl-pyridine ligands where a saturated carbon is inserted between two pyridines of the tpy ligand and was reported in 2004 [49]. Although a pyridine ligand is lower in the spectrochemical series than *e.g.* a bpy ligand, it was believed that the tridentate bipyridyl-pyridine ligands as a whole would exert a stronger ligand field than the pivotal tpy due to a larger bite angle. The ligand **bpy-py** containing a methylene link was obtained via reduction of ketone **bpy-py$_{ket}$** which in turn was prepared from the reaction of 2-lithiopyridine and 6-cyano-2,2′-bipyridine [50] (Scheme 2). The analogous bipyridyl-pyridine ligands **bpy-py$_{MeOH}$** and **bpy-py$_{MeOMe}$** were synthesized from 6-lithio-2,2′-bipyridine and 2-acetylpyridine; a subsequent alkylation of **bpy-py$_{MeOH}$** gave **bpy-py$_{MeOMe}$** [51]. In a later study, the effect of geminal dialkyl substitution on the bridging carbon was examined using ligand **bpy-py$_{Me}$**, which was conveniently obtained by the alkylation of **bpy-py** [52]. Geminal dialkyl substitution stabilizes several types of transition metal complexes [53]. The homo- and heteroleptic Ru^{II} complexes **15**–**20** were prepared in modest to good yields (22–60%) by reacting the ligands with common Ru^{II} precursors according to standard protocols (*c.f.* Scheme 1), either $Ru(ttpy)(DMSO)Cl_2$ or $Ru(DMSO)_4Cl_2$, with one or two equivalents of the ligands in refluxing alcohol or alcohol/H_2O solutions (Scheme 2).

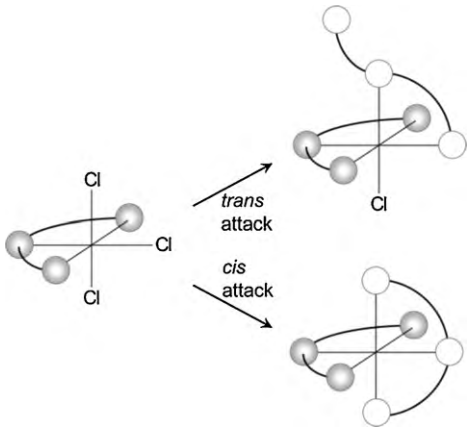

Fig. 6. Initial coordination of a peripheral pyridine unit of tpy at either a *trans* or *cis* position to the central ring of the other tpy ligand leads to $[Ru(N^N^N\text{-tpy})(N^N\text{-tpy})Cl]^+$ and $[Ru(N^N^N\text{-tpy})_2]^{2+}$, respectively.

The initial study of complex **15** indeed showed that the approach is viable to achieve bistridentate complexes with improved geometry [49]. Inspection of the X-ray crystal structure in Fig. 7 reveals larger bite angles of the tridentate ligands compared to $[Ru(tpy)_2]^{2+}$, with N1–Ru1–N3 and N4–Ru1–N6 approximately 168°. Due to the unsymmetrical nature of the tridentate ligands, the complex is chiral (chiral at metal) and was isolated as a racemic mixture. It is best described by the symmetry label C_2 and the two protons on each methylene link are diasterotopic and appear as two doublets in the ^{1}H NMR. The X-ray structures of **16** and **19** also demonstrated that a more ideal bite angle is achieved for different bipyridyl-pyridine ligands (Fig. 7) [51,52], although important differences in the N–Ru–N bond angles and bond distances are evident, most likely as a result of ligand–ligand interactions within the complexes. This is particularly evident in **16** where the ligands adopt bent structures leading to distorted N–Ru–N angles between the lone pyridines (109.7° compared to 98.9° for **15**). In contrast to **15** and **16**, complexes **19** and **20** are chiral as a result of the stereogenic centre in the ligand.

All complexes have ground state properties typical for Ru^{II} polypyridine complexes with reversible redox chemistry and strong absorptions in the visible region of the spectrum due to MLCT transitions involving both the bpy and pyridine parts of the ligands (Table 1). The $Ru^{III/II}$ redox couple is shifted to lower potentials as a result of the mixed bipyridine/pyridine donors

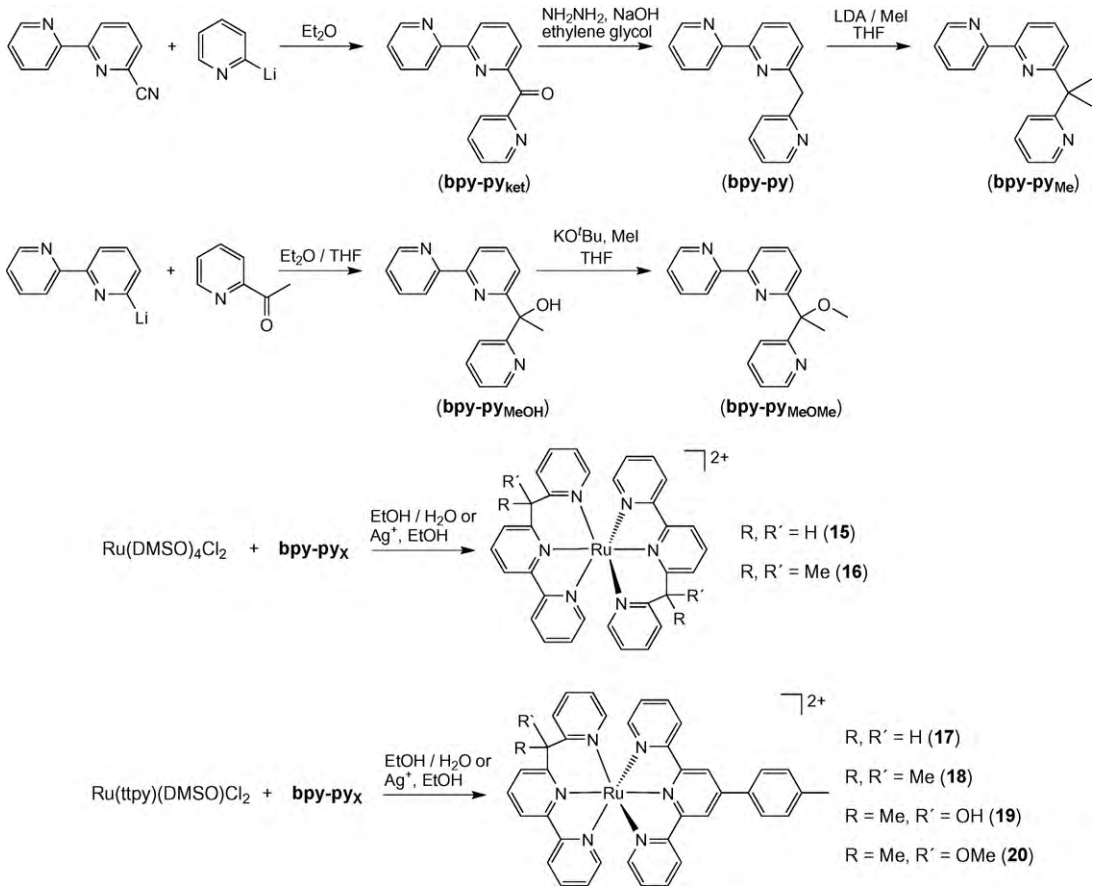

Scheme 2. Synthesis and structures of bistridentate Ru^{II} complexes based on 2,2′-bipyridyl-pyridine ligands bridged by $-CR_2-$ (ttpy is 4′-*p*-tolyl-2,2′:6′,2″-terpyridine).

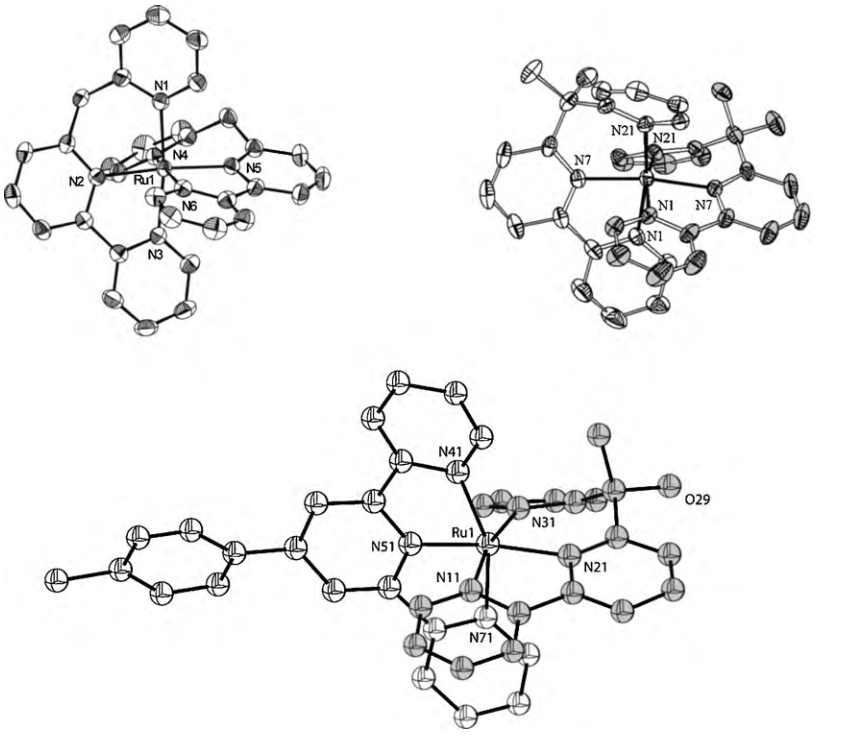

Fig. 7. Top left: ORTEP view of **15** at 30% probability ellipsoids. The N1–Ru1–N3 and N4–Ru1–N6 bite angles are ∼168°; N2–Ru1–N5 is 173.06° and N1–Ru1–N4 is 98.9°. Reproduced by permission of Elsevier from Ref. [49]. Top right: ORTEP view of **16** at 30% probability ellipsoids. N1–Ru–N21: 165.16°, N7–Ru–N7′: 170.61°, N21–Ru–N21′: 109.74°. Reproduced by permission of American Chemical Society from Ref. [52]. Bottom: ORTEP view of **19** at 30% probability ellipsoids. N11–Ru1–N31: 168.5°, N21–Ru1–N51: 172.2°, N31–Ru1–N41: 100.0°. Reproduced by permission of American Chemical Society from Ref. [51].

Table 1
Electrochemical and photophysical data.

Complex[a]	$E_{1/2}$ *vs.* Fc[b]		λ_{max}[c] (nm) ε ($\times 10^{-4}$ $M^{-1}cm^{-1}$)		Emission[d]				
	$Ru^{2+/+}$	$Ru^{3+/2+}$			λ_{max} (nm)	τ (ns)	ϕ_{em}	λ_{max} (nm) 77 K	τ (μs) 77 K
$[Ru(bpy)_3]^{2+}$	−1.74	0.88	450 (1.4)		630[e]	1150[e]	0.089[e]	582[f]	5.2[f]
$[Ru(tpy)_2]^{2+}$[g]	−1.62[h]	0.92[h]	476 (1.8)		–	0.25	–	598	11
$[Ru(ttpy)_2]^{2+}$[g]	−1.62[h]	0.87[h]	490 (2.8)		640[i]	0.95[i]	3.2×10^{-5}[i]	628[i]	9.1[i]
Bipyridyl-pyridine ligands bridged by $-CR_2-$									
15	−1.67	0.78	477 (0.82)		655	15.0	1×10^{-3}	609	3.7
16	−1.64	0.84	472 (0.74)		650	0.3	1×10^{-4}	603	3.5
17	−1.61	0.82	486 (1.5)		655	1.4	2×10^{-4}	637	8.1
18	−1.58	0.82	485 (1.5)		[j]	~0.1	$<2 \times 10^{-5}$	650	5.6
19	−1.60	0.79[k]	482 (1.5)		~655	0.14	$\sim 4 \times 10^{-5}$	650	7.4
20	−1.60	0.81	482 (1.7)		~650	0.47	$\sim 6 \times 10^{-5}$	639	9.2
Polypyridine ligands bridged by –CO–									
21	−1.13	0.95	474 (0.87)		[l]	[l]	[l]	696	1.9 (75%)5.8 (25%)
22	−1.02	0.98	536 (0.50)	451 (0.91)	796[b]	[l]	1.30×10^{-4}[b]	[l]	[l]
23	−0.91	1.09	549 (0.56)		772[b]	[l]	1.77×10^{-4}[b]	[l]	[l]
24	−1.33[m]	1.10[m]	562 (0.26)	522 (0.64)	608[b]	3300[b] 1360[b,n]	0.3[b] 0.13[b,n]	613[o]	6.43[o] 6.17[n,o]
A phenanthrolinyl-quinoline ligand									
25	−1.49	0.78	485 (1.0)		712	810	5×10^{-3}	672	4.1
Diquinolinyl-pyridine ligands									
26	−1.73	0.71	491 (1.4)		700	3000	0.02	673	8.5
27	−1.73	0.64	552 (1.1)		694[b]	2300[b]	0.04[b]	[l]	[l]
28	−1.76	0.56	502 (1.0)		718	1200	0.005	[l]	[l]
29	−1.52	0.82	553 (1.0)	488 (1.1)	693	5500	0.07	661	11.2
30	−1.86	0.34	563 (0.8)	476 (1.1)	~780	450	4×10^{-4}	726	2.7
31	−1.58	0.77	549 (0.7)	492 (1.0)	706	4300	0.04	672	10.7
32	−1.75	0.63	498 (1.2)		702	2000	0.01	[l]	[l]
33	−1.71	0.69	496 (1.4)		690	3000	0.03	[l]	[l]
34	−1.62	0.73	492 (1.2)		693	2900	0.02	[l]	[l]
35	−1.65	0.57	521 (1.1)		741	2000	0.02	[l]	[l]
36	−1.66	0.65	510 (1.0)		759	500	0.003	[l]	[l]

[a] As PF_6^- salt.
[b] MeCN.
[c] MeCN. Only the MLCT band of lowest energy, unless prominent shoulders are reported.
[d] EtOH/MeOH, at RT and at 77 K.
[e] Data from Ref. [8].
[f] Data from Ref. [81], Cl^- salt.
[g] Data from Ref. [11].
[h] Reported *vs.* SSCE. 0.38 V subtracted to obtain values *vs.* Fc.
[i] Nitrile solvents.
[j] Very weak emission centered around 650–700 nm.
[k] Anodic peak potential.
[l] Not reported.
[m] Reported *vs.* Ag/AgCl. 0.425 V subtracted to obtain values *vs.* Fc.
[n] Aerated conditions.
[o] Propionitrile/butyronitrile.

but the effect is rather small. More apparent is the difference in intensity of the MLCT transitions at around 470–490 nm between homoleptic **15**–**16** and heteroleptic **17**–**20** as a result of the ttpy ligand (ttpy is 4′-*p*-tolyl-2,2′:6′,2″-terpyridine) in the latter complexes which increases the transition dipole moment [14]. An unusual redox behavior was however observed for **19**, where the ambidentate nature of the tridentate ligand leads to a change in coordination from N_6 in Ru^{II} to N_5O in Ru^{III}. This linkage isomerization reaction is reversible with similar rate-constants for both the forward ($Ru^{III}N_6 \rightarrow Ru^{III}N_5O$, $k = 2.5 \times 10^2$ s^{-1}) and the backward ($Ru^{II}N_5O \rightarrow Ru^{II}N_6$, $k = 8 \times 10^2$ s^{-1}) reaction and the process in this and related complexes has been studied in some detail [54,55].

Luminescence properties for **15**–**20** are reported in Table 1. In contrast to $[Ru(tpy)_2]^{2+}$, all complexes are weakly emitting at room temperature. The luminescence properties for **17**–**20**, including the 77 K luminescence, are similar to the weakly emitting $[Ru(ttpy)_2]^{2+}$ and was therefore attributed to a ^{3}MLCT excited state localized on the ttpy ligand. Temperature-dependent emission measurements confirmed that thermally activated decay via ^{3}MC states is a rapid process in **17**–**20**, and the apparent benefit of a more octahedral coordination is offset by a distorted geometry as a consequence of the bridge substituents. Only for **17**, where such substituents are absent, the excited state lifetime is longer than for $[Ru(ttpy)_2]^{2+}$.

The excited state lifetime for the homoleptic **15** is 15 ns with a concomitant increase in luminescence quantum yield. Temperature-dependent emission measurements showed that thermally activated decay via ^{3}MC states is indeed considerably suppressed giving an activated rate-constant ($k_{nr}^{act} = Ae^{-\Delta E/RT}$) which is an order of magnitude smaller than for $[Ru(tpy)_2]^{2+}$. At the same time, the ^{3}MLCT excited state energy is only marginally affected and the 4-positions on the central pyridines are unsubstituted which allow for the use of these complexes in linear multicomponent assemblies. In contrast to **15**, the room temperature luminescence properties for **16** are poor and the complex exhibits an excited state lifetime of 0.3 ns (Table 1). This was explained by the structural distortion seen in the X-ray crystal structure (and confirmed by DFT calculations) due to the bridge substituents [52], leading to a weak ligand field and therefore rapid excited state decay via the ^{3}MC state. In the calculated energy diagrams for **15** and **16** shown in Fig. 8, it is clear that the lowest ^{3}MLCT

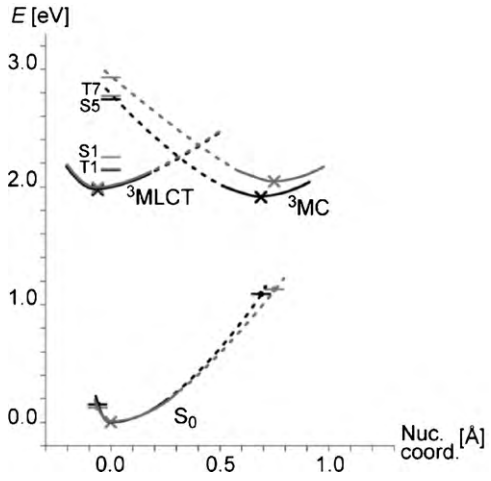

Fig. 8. Calculated energy diagram of **15** (grey) and **16** (black). The total energies of the DFT optimized states, i.e. the S_0, ^{3}MLCT, and ^{3}MC states are denoted by crosses. Vertical single-point energies of the S_0 surface for the ^{3}MLCT and ^{3}MC geometries are indicated by dots on a horizontal bar. Vertical singlet and triplet excitation energies of the S_0 state are shown as horizontal bars and denoted as follows: T1 is the lowest vertical singlet–triplet transitions from S_0 to a ^{3}MLCT surface and T7 the lowest vertical singlet–triplet excitation from S_0 to a ^{3}MC surface. S1 is the lowest singlet–singlet transition of MLCT character, and S5 the lowest singlet–singlet transition of MLCT character with a significant oscillator strength. Reproduced by permission of American Chemical Society from Ref. [52].

states for both complexes are similar in energy which agrees well with the experimental findings. However, a significant difference for the ^{3}MC states is evident, where the ^{3}MC state for **16** is even lower than the ^{3}MLCT state. This leads to a lowering of the activation barrier for the ^{3}MLCT to ^{3}MC conversion which accounts for the short excited state lifetime in **16**.

4.2. Polypyridine ligands bridged by –CO–

Complex **21**, containing the keto-functionalized ligand **bpy-py$_{ket}$**, was part of our original study on the bipyridyl-pyridine ligands and their Ru^{II} complexes [51]. It was prepared in 28% yield from Ru(ttpy)(DMSO)Cl$_2$ and **bpy-py$_{ket}$** (Scheme 3). As expected, due to the electron-withdrawing carbonyl, the complex is more difficult to oxidize than analogous complexes based on the bipyridyl-pyridine ligands and much more easily reduced. The electron-withdrawing carbonyl stabilizes the ligand-based LUMO more than it destabilizes the metal-based HOMO. This is mirrored in the absorption spectrum which shows broad and red-shifted MLCT transitions although the peak maximum is at 474 nm (Table 1). The luminescence properties are poor however, which precluded an accurate determination of the excited state lifetime at room temperature.

Bark and Thummel described similar Ru^{II} complexes **22** and **23** based on the keto-functionalized ligand **phen-py$_{ket}$** in 2005 (Scheme 3) [56]. The ligand was obtained employing the Friedländer methodology reacting 8-amino-7-quinolinecarbaldehyde with oxime-derivatized pyrid-2-yl acetone followed by oxidative cleavage of the oxime to give **phen-py$_{ket}$** (Scheme 3). The heteroleptic complex **22** and homoleptic **23** were obtained in 42% and 78% yields, respectively, using standard reaction conditions. Similar to **15** and **16**, complex **23** is chiral due to two unsymmetrical tridentate ligands and the complex was isolated as a racemic mixture. Although the excited state lifetimes were not reported for **22** and **23**, both complexes are emissive at room temperature with luminescence maxima at 796 nm and 772 nm, respectively (Table 1). This was attributed to a stronger ligand field than in $[Ru(tpy)_2]^{2+}$ due to decreased strain using the **phen-py$_{ket}$** ligands. Consistent with such an interpretation is the fact that the homoleptic complex **23** is a stronger emitter even though the luminescence maximum is shifted to higher energy compared to the heteroleptic complex **22**.

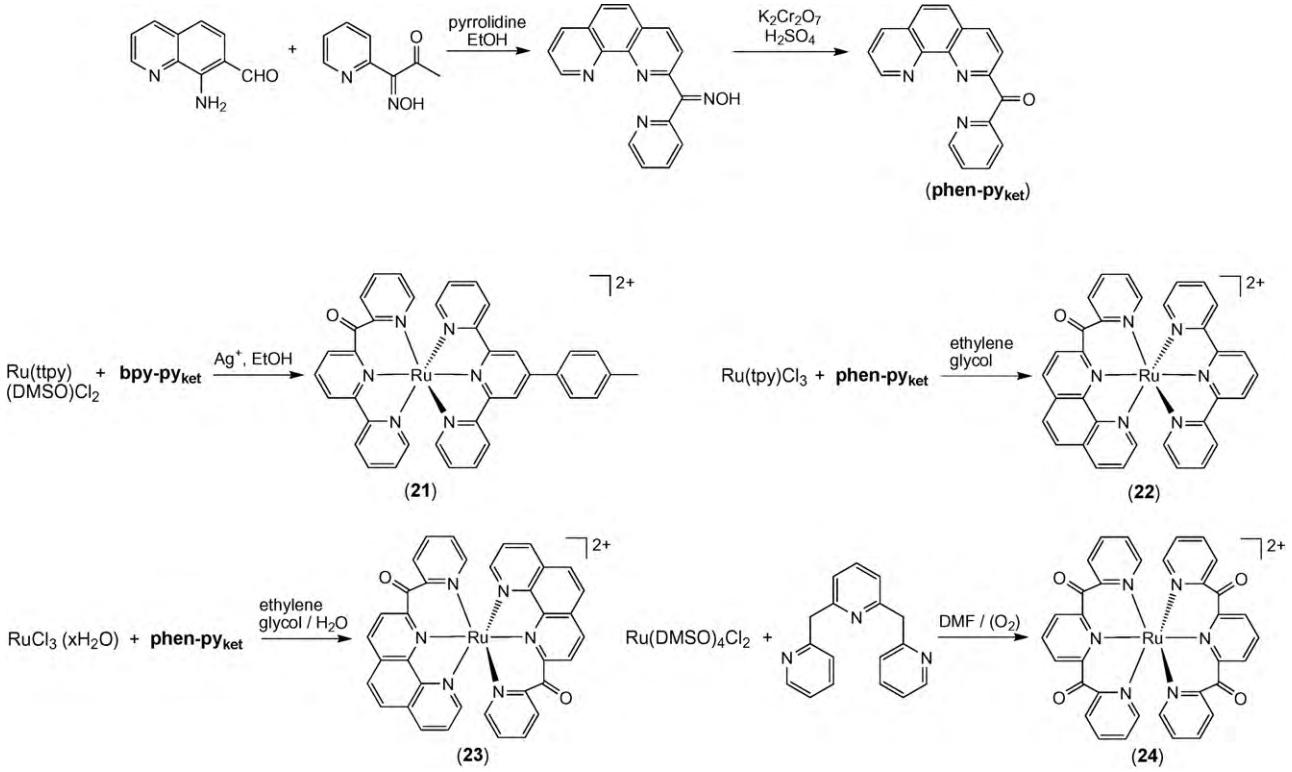

Scheme 3. Synthesis and structures of bistridentate Ru^{II} complexes based on polypyridine ligands bridged by –CO–.

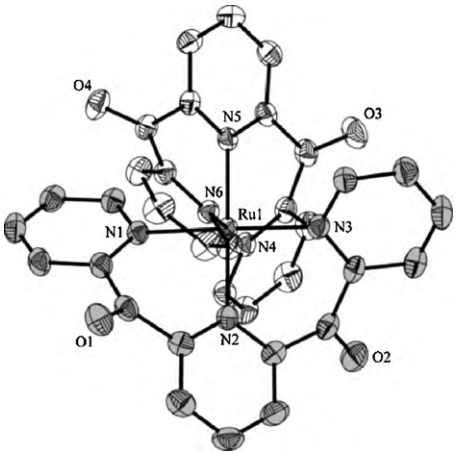

Fig. 9. ORTEP view of **24** at 50% probability ellipsoids. N1–Ru1–N3: 177.77°, N2–Ru1–N5: 179.19°. Reproduced by permission of American Chemical Society from Ref. [57].

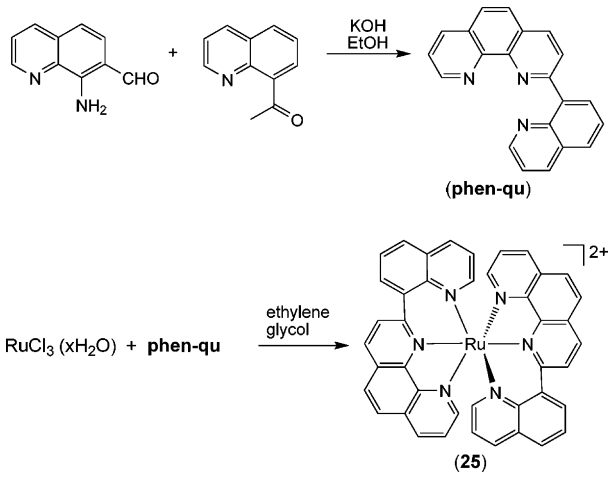

Scheme 4. Synthesis and structure of **25** containing a phenanthrolinyl-quinoline ligand.

More recently Fliegl, Keyes, and Ruben and co-workers reported in 2009 the tetra-keto-functionalized bistridentate Ru^{II} complex **24** (Scheme 3) [57]. 2,6-Di(pyrid-2-yl-methyl)pyridine [58] was heated with $Ru(DMSO)_4Cl_2$ and generated **24** in 10% yield after *in situ* air oxidation. Interestingly, initial oxidation of the ligand and attempted coordination to Ru^{II} using $Ru(DMSO)_4Cl_2$ failed to give **24**. The complex shows close to ideal octahedral geometry with similar Ru–N bond lengths as a result of the inserted –CO– units between the pyridine rings of the tridentate ligands (Fig. 9). As has been noted before in metal complexes based on this ligand [59], it adopts a helical conformation leading to (λ,λ) and (δ,δ) enantiomers of the Ru^{II} complex. The helical conformation of the ligand leads to an almost perpendicular orientation of the peripheral pyridine rings on each ligand (Fig. 9).

Complex **24** shows broad absorption in the visible spectroscopic region assigned to MLCT transitions which was supported by TD-DFT calculations (Fig. 10). The emission is intense, both at room temperature and at 77 K, with excited state lifetimes as long as 3.30 μs and 6.43 μs (in deaerated solutions), respectively. Although the excited state energy is high (λ_{em} = 608 nm), the difference in excited state lifetime at room temperature and at 77 K is only a factor 2, suggesting that deactivation via the ^{3}MC state is suppressed due to the strong ligand field in the octahedral complex. Also of interest is the high quantum yield of emission which is unusually high for a Ru^{II} polypyridine complex and is little affected by the presence of oxygen (Table 1). At room temperature, the complex

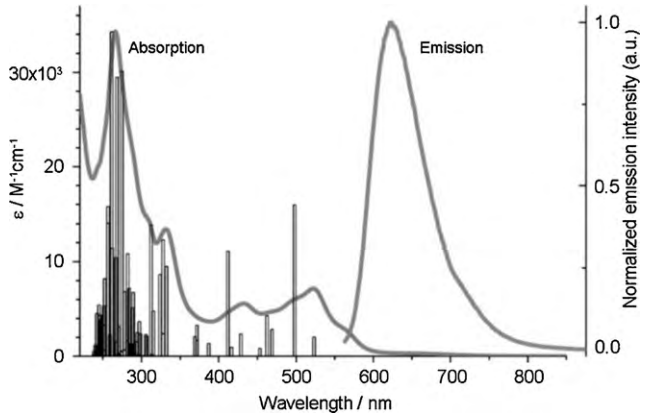

Fig. 10. Absorption and emission spectra of **24** (air-equilibrated MeCN). Bars represent the calculated absorption spectrum. Reproduced by permission of American Chemical Society from Ref. [57].

exhibits ϕ_{em} = 0.3 in deaerated solution which drops to ϕ_{em} = 0.13 in the presence of oxygen. The high quantum yield of emission was attributed to a small non-radiative decay rate (k_{nr}) due to a small displacement between the excited state and the ground state structures. This conclusion was supported by spectroscopic fitting of the low-temperature emission data. However, a number of observations were reported that are uncharacteristic for ^{3}MLCT states of Ru^{II} polypyridine complexes. (i) The emission maximum does not blue shift in a 77 K glass, (ii) the emission lifetime is influenced very little by oxygen, and (iii) the apparent Stokes shift between the lowest ^{1}MLCT charge transfer absorption band and the emission maximum is very small. The authors noted that although the calculations suggest ^{3}MLCT character, a ^{3}LC contribution to the emission cannot be excluded.

4.3. A phenanthrolinyl-quinoline ligand

Thummel and Hammarström and co-workers reported in 2007 a set of Ru^{II} complexes combining pyridine/phenanthroline units with quinoline [60]. When the quinoline ring is linked in the 8-position to the *ortho* position of the nitrogen in the other heterocycle, a 1,5-relationship between the two nitrogen donor atoms is created which leads to a 6-membered chelate upon coordination. One of the complexes (**25**) was a bistridentate complex containing ligands with expanded "tpy" cores (Scheme 4). The ligand **phen-qu** was obtained through a Friedländer condensation of 8-amino-7-quinolinecarbaldehyde with 8-acetylquinoline [61]. Heating the ligand with $RuCl_3 \cdot xH_2O$ in ethylene glycol gave **25** in 36% yield.

The geometry of **25** was optimized using DFT calculations which showed bite angles close to 180° with the quinoline moiety twisted about 27° out of the phenanthroline plane. The complex is luminescent at room temperature with a ^{3}MLCT excited state lifetime of 810 ns (Table 1). However, the emission energy (λ_{em} = 712 nm) is significantly lower compared to $[Ru(tpy)_2]^{2+}$. To establish that the increase in lifetime is an effect of a stronger ligand field and not just a consequence of the lower energy of the ^{3}MLCT state, temperature-dependent emission measurements were carried out and the results compared to those for similar complexes. It was concluded that the longer ^{3}MLCT excited state lifetime observed for **25** can be attributed to a stronger ligand field due to more octahedral coordination.

4.4. 2,6-Di(quinolin-8-yl)pyridine ligands

Following our earlier work on the bipyridyl-pyridine ligands, we became interested in ligands where the saturated carbon is

removed from the 6-membered chelate ring. It was believed that a ligand that contained only aromatic units would lead to more rigid structures. Initial DFT calculations on a homoleptic complex based on 2,6-di(quinolin-8-yl)pyridine (**dqp**) showed bite angles close to 180° with regular Ru–N bond distances (Fig. 11) [62]. The calculations also confirmed that the HOMO is metal-centered while the LUMO is ligand-centered and extends over the entire tridentate ligand although a twisted ligand orientation is apparent. The LUMO also has a significant contribution at the C^4 position of the central pyridine which may be of importance for efficient quenching in donor–acceptor systems. In 2006, we subsequently presented the first study of the corresponding homoleptic Ru^{II} complex (**26**) where the geometry was very close to the predicted structure, and which displayed a remarkably long ^{3}MLCT excited state lifetime of 3.0 μs (ϕ_{em} = 0.02) [62]. X-ray analysis of **26** confirmed *mer* coordination of the dqp ligands with a very close to ideal geometry, the N1–Ru1–N3 and N4–Ru1–N6 bite angles are ~178°. The ligands adopt helical arrangements with dihedral angles between the central pyridine and quinoline units that are 35–39°, an arrange-

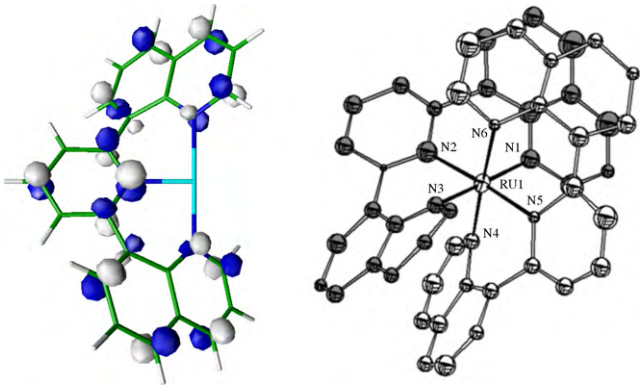

Fig. 11. DFT calculation of the LUMO orbital in **26** (one ligand omitted for clarity). Right: ORTEP view of **26** at 50% probability ellipsoids showing almost ideal bite angles (N1–Ru1–N3 and N4–Ru1–N6 bite angles are ~178°). Reproduced by permission of American Chemical Society from Ref. [62].

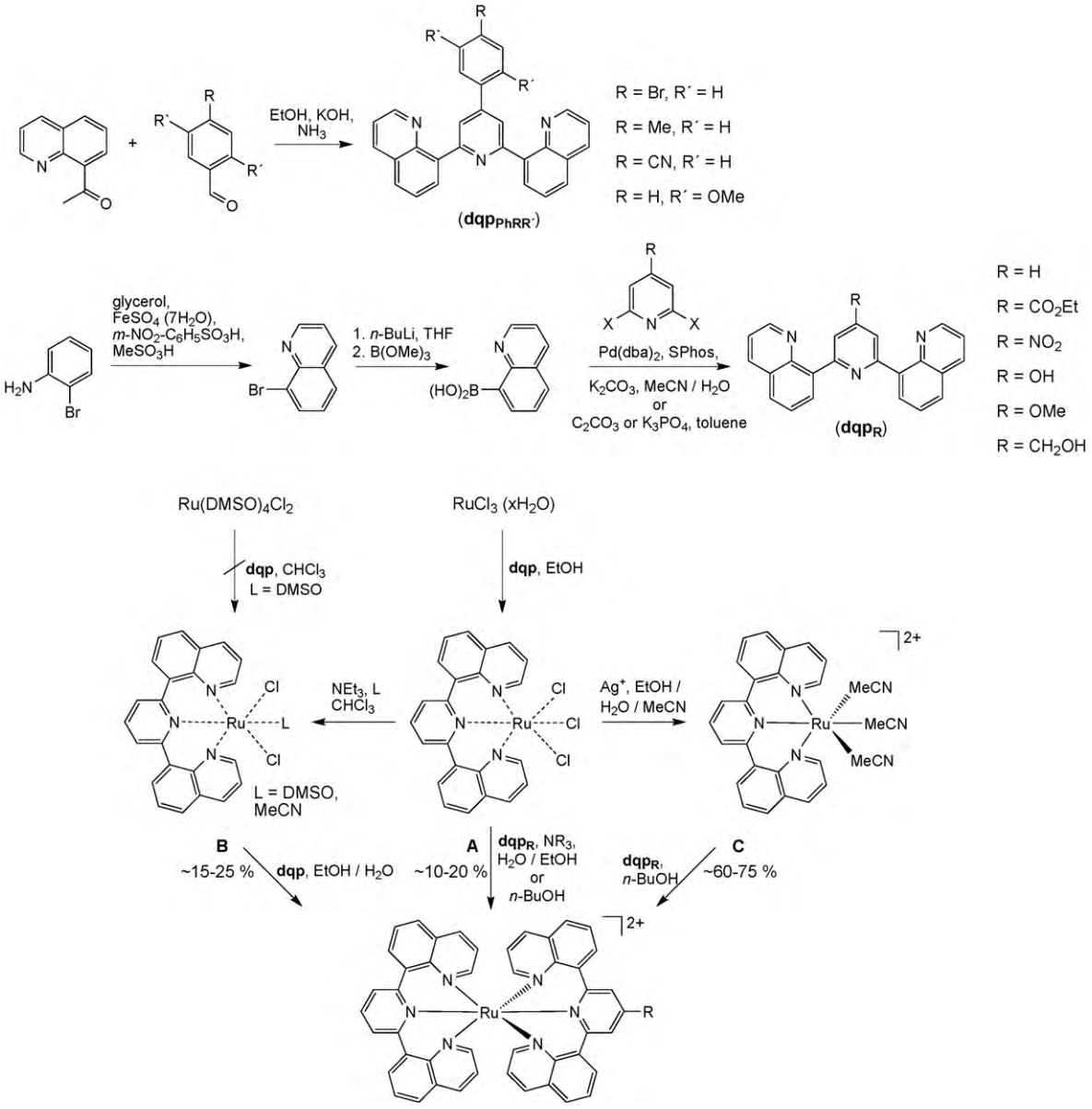

Scheme 5. Synthesis of dqp ligands (top) and stepwise coordination of dqp ligands to Ru (bottom). Different [Ru(**dqp$_R$**)(MeCN)$_3$]$^{2+}$ precursors (R = –H, –OH, –CO_2Et) have been prepared and used in the synthesis of heteroleptic complexes.

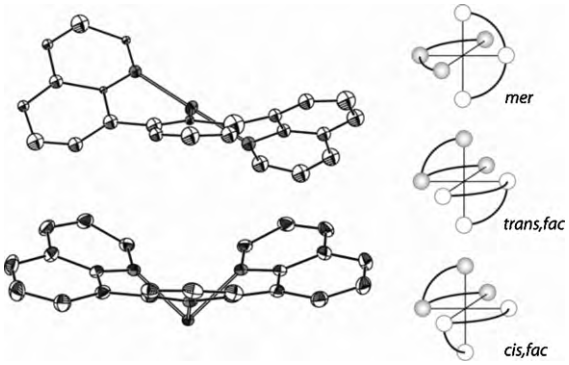

Fig. 12. ORTEP views (40% probability ellipsoids) showing ligand orientations in **26** (top) and the *trans,fac* isomer (bottom), one ligand omitted for clarity. Reproduced by permission of American Chemical Society from Ref. [63]. Schematic representations of the three isomers where the *trans*/*cis* notation refers to the relative positions of the pyridine units.

ment which leads to intramolecular stacking between quinoline units. Such interligand π–π interactions were also observed by ^{1}H NMR in solution, but it has most likely a minor role in stabilizing the structure since the dqp ligand adopts a similar helical twist in [Ru(**dqp**)(MeCN)$_3$]$^{2+}$ [63]. The induced helical arrangement of the ligands makes the complex chiral (best described by symmetry label D_2) where one ligand sets the conformation of the other (either λ,λ or δ,δ conformations). Before discussing the photophysical properties of these complexes, the synthesis of the dqp ligands and their Ru^{II} complexes will be reviewed.

4.4.1. Preparation of dqp ligands and Ru^{II} complexes

The synthesis of the dqp ligands is based on strategies developed for tpy [64–66]. Several synthetic approaches to tpy ligands have been presented, either through coupling methodologies of pyridine derivatives or through condensation reactions forming pyridine rings. Applying the one-step synthesis presented by Wang and Hanan for tpy [67], the aryl-susbtituted dqp ligands shown in Scheme 5 were obtained from 8-acetylquinoline [68] and commercially available arylaldehydes [69]. The yields (23–35%) are consistently lower than for tpy, but provide rapid access to this class of ligands. A Pd-catalyzed cross-coupling strategy was also explored, utilizing Suzuki conditions and quinolin-8-yl boronic acid. Although Suzuki conditions have been of limited use for tpy due to problems associated to instability and facile protodeboronation of pyrid-2-yl boronic acids [70], the Suzuki reaction is advantageous compared to the Stille reaction due to the toxic byproducts formed using the latter protocols. Using quinolin-8-yl boronic acid and 2,6-dihalo substituted pyridines in either aqueous or non-aqueous solvents, a variety of 4-substituted dqp ligands were obtained. An aqueous system is particularly convenient for R = –H, –OH, and –OMe which, using microwave-assisted heating at 120–140°, provides rapid access to the corresponding dqp ligands in 70–80% yields [71]. 8-Bromoquinoline and quinolin-8-yl boronic acid are commercially available but at a rather high cost, however, they can be easily prepared in a multi-gram scale relying on a large-scale Skraup reaction as described by Conlon and co-workers [72]. The amino- and the bromo-functionalized dqp ligands were also prepared using standard functional group interconversion [69].

Initial synthesis of homoleptic Ru^{II} complexes relied on microwave-assisted heating at 196° to provide **26** in 87% yield [62]. These conditions were convenient for thermally stable dqp ligands (*e.g.* complexes **27** and **28**, Fig. 14), but failed for ligands containing sensitive functional groups. Interestingly, applying less drastic conditions in the synthesis of **26** led to the formation of the kinetically favored *fac* isomers *trans*,*fac*-**26** and *cis*,*fac*-**26** (Fig. 12) which

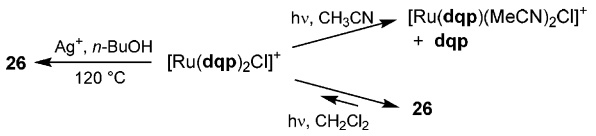

Fig. 13. Photochemical conversion of [Ru(N^N^N-**dqp**)(N^N-**dqp**)Cl]$^+$ to **26** in CH_2Cl_2. The complex is also converted to **26** using Ag^+ in *n*-BuOH.

were thermally converted to the thermodynamically favored *mer* isomer **26** [63].

In our efforts to develop a general and mild strategy for the synthesis of homo- and heteroleptic Ru^{II} complexes, the dqp ligands were found to have distinct reactivity compared to the related tpy ligands [63]. Neither using the Ru(**dqp**)Cl$_3$ precursor (route A, Scheme 5) nor a Ru(**dqp**)XCl$_2$ precursor (route B) provided the desired products in high yields (*c.f.* Scheme 1). Structurally uncharacterized [Ru(N^N^N-**dqp**)(N^N-**dqp**)Cl]$^+$ was the major product, which, in analogy to tpy complexes [47], could be photochemically converted to the desired *mer* complex **26** in low-coordinating CH_2Cl_2 (Fig. 13). Instead, [Ru(**dqp$_R$**)(MeCN)$_3$]$^{2+}$ complexes (route C, Scheme 5) proved to be versatile intermediates and allowed the facile preparation of (*mer*)**29**-**36** (Fig. 14), generally in good yields (up to 75%). X-ray diffraction of [Ru(**dqp**)(MeCN)$_3$]$^{2+}$ confirmed *mer* coordination of the tridentate ligand [63]. Interestingly, the synthesis of Ru(**dqp**)(DMSO)Cl$_2$ from Ru(DMSO)$_4$Cl$_2$ was not achievable using the conditions developed for tpy. Instead, based on NMR coupling constants and LC–MS analysis, the species obtained was assigned to a pyridine mono-coordinated complex, [Ru(**dqp**)(DMSO)$_4$Cl]$^+$, with two non-coordinating quinoline units. Similar mono-coordinated complexes based on Ir have been observed [73], indicating that dqp ligands, in contrast to tpy, initially coordinates via the central pyridine with subsequent formation of the metal-quinoline bonds.

4.4.2. Electrochemical and photophysical properties of dqp Ru^{II} complexes

All dqp Ru^{II} complexes **26**–**36** examined to date exhibit strong ^{1}MLCT transitions in the visible part of the spectrum (Fig. 15), and have ^{3}MLCT excited state luminescent lifetimes on the order of a few μs (0.45–5.5 μs) (Table 1) [62,63,74]. The complex that currently shows the longest excited state lifetime and highest quantum yield of emission is **29** containing two electron-withdrawing –CO_2Et substituents (τ = 5.5 μs, ϕ_{em} = 0.07). The assignment of the lowest excited state to ^{3}MLCT was based on a number of experimental observations. (i) The *in situ* prepared [Zn(**dqp**)$_2$]$^{2+}$ complex exhibits ligand-based fluorescence

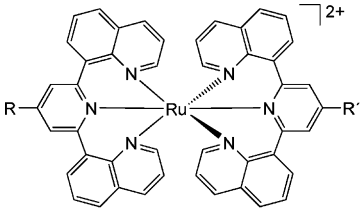

R, R′ = H (**26**)
R, R′ = *p*-tolyl (**27**)
R, R′ = OMe (**28**)
R, R′ = CO_2Et (**29**)
R, R′ = NH_2 (**30**)
R = H, R′ = CO_2Et (**31**)
R = H, R′ = OMe (**32**)
R = H, R′ = PhBr (**33**)
R = H, R′ = Br (**34**)
R = CO_2Et, R′ = NH_2 (**35**)
R = OH, R′ = Br (**36**)

Fig. 14. Structures of *mer* dqp-based Ru^{II} complexes.

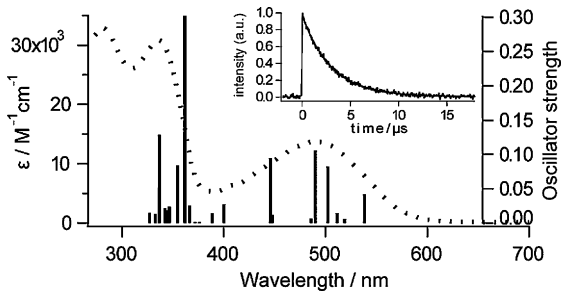

Fig. 15. Measured (dotted line, MeCN) and calculated (bars, EtOH) absorption spectrum of **26**. Inset: Emission decay at room temperature in deaerated EtOH/MeOH. Reproduced by permission of American Chemical Society from Ref. [62].

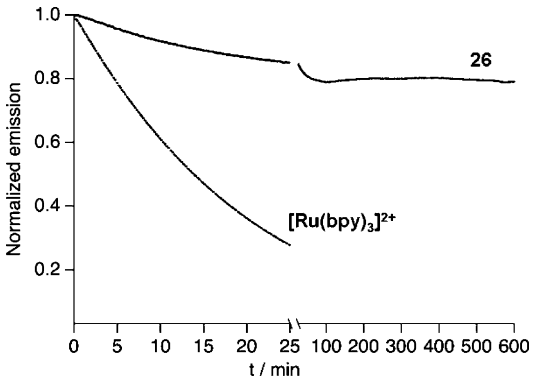

Fig. 16. Photostability experiments of **26** and $[Ru(bpy)_3]^{2+}$ (CH_2Cl_2, 2 mM TBACl). Reproduced by permission of American Chemical Society from Ref. [74].

and phosphorescence at higher energy (zero–zero transitions at $\lambda_{em} \sim 370$ and 490 nm, respectively). (ii) Transient absorption data and low-temperature emission spectra are typical for Ru^{II} polypyridine complexes. (iii) The luminescence maxima shift in parallel to the difference in electrochemical potentials for the metal oxidation and first ligand reduction, and (iv) DFT calculations on **26** are consistent with a metal-centered HOMO and a ligand-centered LUMO. The excited state energies for the dqp-based complexes are somewhat lower than for related Ru^{II} polypyridine complexes. This is due to an ~0.2 V anodic shift of the $Ru^{III/II}$ redox couple compared to similar Ru^{II} polypyridine complexes and was attributed to less efficient π back-bonding in dqp-based Ru^{II} complexes considering the similar pK_a values for quinoline and pyridine [74]. The ^{3}MLCT excited state lifetimes at 77 K measured for a selection of complexes are typical for Ru^{II} polypyridine complexes. The comparably small difference in excited state lifetime at room temperature and at 77 K indicates that the more octahedral coordination efficiently blocks deactivation via ^{3}MC states due to stronger ligand fields. This is supported by the fact that **26** exhibits an excited state lifetime of 1.3 µs even at 363 K where $[Ru(bpy)_3]^{2+}$ displays a lifetime of only *ca.* 100 ns [75].

Analysis of the emission decay in **26** revealed a radiative decay rate which is an order of magnitude lower than usually observed for ^{3}MLCT emitters ($k_r = 7 \times 10^3\ s^{-1}$). Also the non-radiative rate-constant (k_{nr}) is lower than expected based on energy gap law arguments. This accounts for the long excited state lifetimes of this class of photosensitizers, and efforts to explain these observations are currently pursued in our laboratories [76].

5. Photochemistry of dqp Ru^{II} complexes and intramolecular charge separation in D–P–A assemblies

Photosubstitution reactions on $[Ru(bpy)_3]^{2+}$ are efficient in CH_2Cl_2 in the presence of strong nucleophiles due to thermal population of the ^{3}MC state leading to ligand loss as a consequence of the antibonding character of the e_g orbitals [77]. In view of these results, photostability experiments were performed on complex **26** which initially showed no degradation in EtOH/MeOH solutions. Using the typical conditions for photosubstitution on $[Ru(bpy)_3]^{2+}$ (CH_2Cl_2 with excess Cl^-), it was demonstrated that **26** is much more stable than $[Ru(bpy)_3]^{2+}$ as would also be expected due to the tridentate nature of the dqp ligands [74]. Interestingly, a photostationary state is formed in which 80% of the initial emission intensity remains even after >12 h of irradiation (Fig. 16). In comparison, the decomposition half-life of $[Ru(bpy)_3]^{2+}$ was determined to be 14 min. This observation was explained by the photochemical conversion of [Ru(N^N^N-**dqp**)(N^N-**dqp**)Cl]$^+$ to **26** (Section 4.4, Fig. 13), the former which is presumably the same intermediate formed in the photostability experiments.

Complex **26** functions as photosensitizer in bimolecular electron/energy transfer reactions with common organic quenchers (Eqs. (2)–(4)) [74]. The reactions are efficient in MeCN with second-order quenching rate-constants that are close to diffusion controlled for reductive quenching by TTF (tetrathiofulvalene) and energy transfer quenching by DPA (diphenylantracene), while somewhat slower for oxidative quenching to MV^{2+} (methyl viologen).

$$^3[Ru(\mathbf{dqp})_2]^{2+} + TTF \rightarrow [Ru(\mathbf{dqp})_2]^{+} + TTF^{+} \quad 9.9 \times 10^9\ M^{-1}\ s^{-1} \tag{2}$$

$$^3[Ru(\mathbf{dqp})_2]^{2+} + DPA \rightarrow [Ru(\mathbf{dqp})_2]^{2+} + {}^3DPA \quad 3.4 \times 10^9\ M^{-1}\ s^{-1} \tag{3}$$

$$^3[Ru(\mathbf{dqp})_2]^{2+} + MV^{2+} \rightarrow [Ru(\mathbf{dqp})_2]^{3+} + MV^{+} \quad 0.33 \times 10^9\ M^{-1}\ s^{-1} \tag{4}$$

Recently, triads **39** and **40** and the corresponding dyads **37** and **38** were synthesized to demonstrate the utility of dqp Ru^{II} complexes in linear D–P–A arrays for vectorial intramolecular electron transfer (Scheme 6) [78]. The dqp ligands, either functionalized with a quinone precursor (MeQ) or a phenothiazine (PTZ) electron donor, were synthesized using the developed protocols described in Scheme 5. Ligand $\mathbf{dqp_{PhMeQ}}$ was obtained in 61% yield in a Pd-catalyzed Suzuki reaction with a preformed dqp ligand and 2,5-dimethoxyphenylboronic acid, while $\mathbf{dqp_{MeQ}}$ was synthesized in two steps from 2,6-dichloroisonicotinic acid and 2,5-dimethoxybenzylamine in 57% yield. Ligand $\mathbf{dqp_{PTZ}}$ in turn was obtained in 37% yield over three steps through an initial Suzuki coupling of 2,6-dichloro-4-hydroxymethylpyridine [79] and quinolin-8-yl boronic acid. The formed hydroxymethyl functionalized dqp ligand was subsequently subjected to bromination and substitution with deprotonated PTZ. Once the ligands were obtained, the complexes were prepared using the stepwise protocol described in Scheme 5 via $[Ru(\mathbf{dqp_R})(MeCN)_3]^{2+}$ intermediates with initial coordination of **dqp** or the dimethoxyphenyl functionalized dqp ligands. Coordination of the second ligand and subsequent deprotection/oxidation of the fully assembled complexes gave the final dyads and triads shown in Scheme 6. The reaction scheme shown in Fig. 17 (for complex **40**) was constructed from electrochemical data which revealed little interaction between the units.

The electron transfer products following excitation of the Ru^{II} units were followed by transient absorption spectroscopy, monitoring the changes in absorption at different times after excitation. For dyads **37** and **38**, only ^{3}MLCT excited state features were observed which decayed with the same lifetime (~1 ns) as that observed in emission measurements (Table 2). It was concluded that the charge recombination rates (Ru^{III}-$Q^- \rightarrow Ru^{II}$-Q) are much

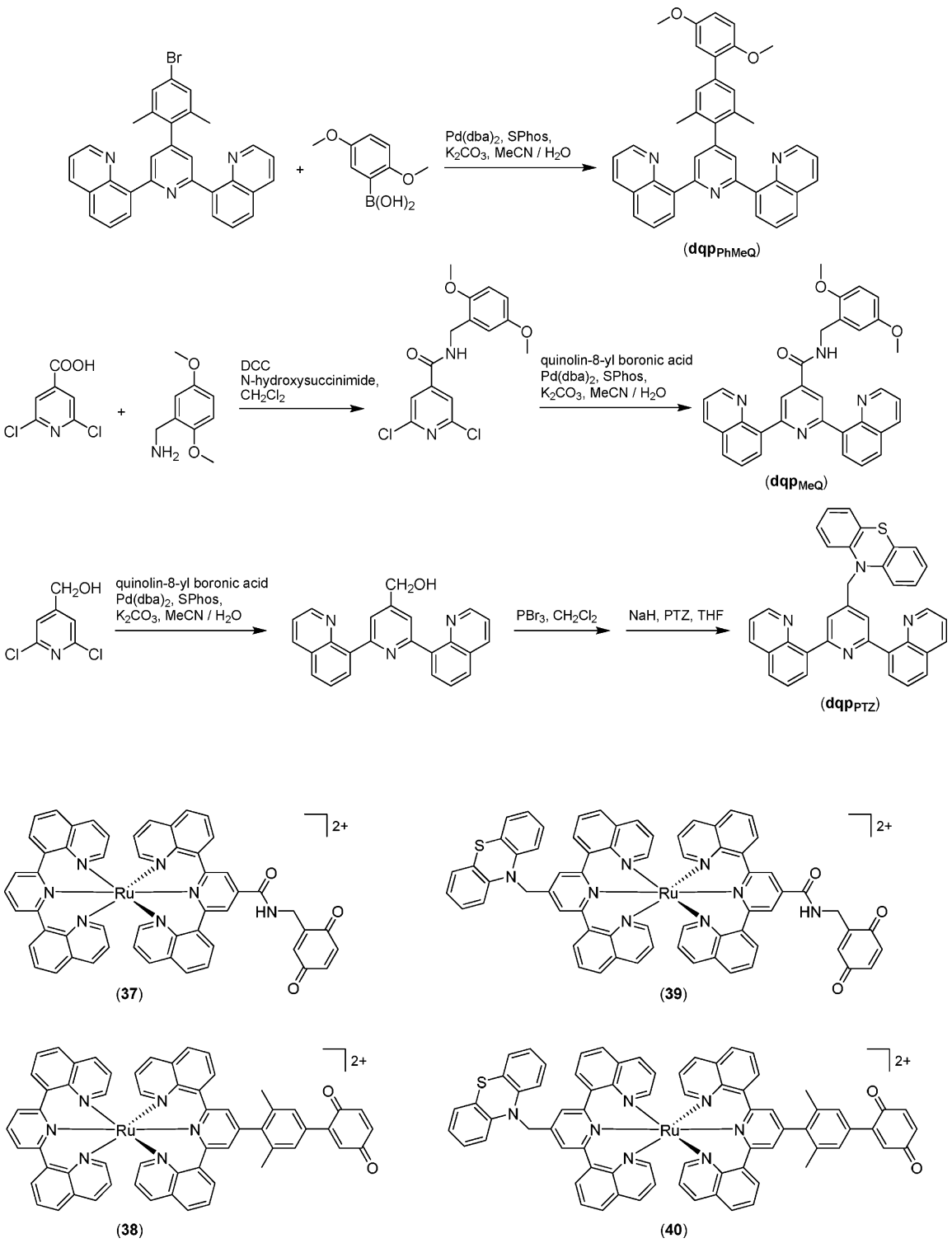

Scheme 6. Synthesis of functionalized dqp ligands and the corresponding dyads and triads.

Table 2
Electron transfer data at 298 K in MeCN.

Complex	Electron transfer		ϕ_{CS}
	k_{CS} (s^{-1})	k_{CR} (s^{-1})	
37	5.1×10^8	$\gg 5 \times 10^8$	≥99%
38	1.1×10^9	$\gg 1 \times 10^9$	≥99%
39	5.2×10^8	7.1×10^6	≥95%
40	1.0×10^9	5.0×10^6	≥50%

higher than the forward electron transfer reaction, thereby precluding detection of the charge-separated states.

For triads **39** and **40**, features of the fully charge-separated state (PTZ^+-Ru^{II}-Q^-) developed within $\tau \sim 1$ ns and decayed with $k_{CR} = 7.1 \times 10^6\ s^{-1}$ and $k_{CR} = 5.0 \times 10^6\ s^{-1}$ for **39** and **40**, respectively (Fig. 17). The kinetics of the charge recombinations (PTZ^+-Ru^{II}-$Q^- \rightarrow$ PTZ-Ru^{II}-Q) are monoexponential as a consequence of the well-defined donor–acceptor distance stemming from the bistridentate Ru^{II} unit. By comparing with the results from the dyads,

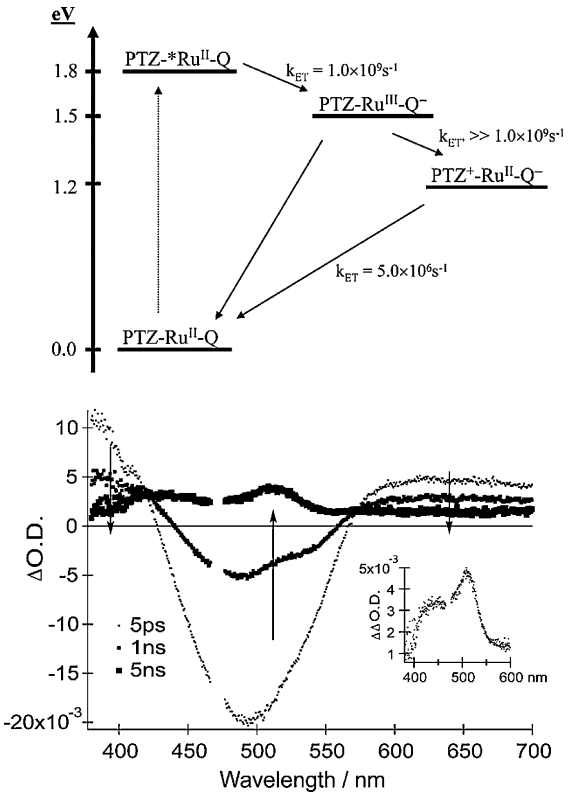

Fig. 17. Top: Reaction scheme and rate-constants determined for complex **40**. Bottom: Transient absorption spectra at different times after the initial excitation (MeCN, 298 K). Inset shows the spectrum after 5 ns, after substraction of excited state features due to unreactive Ru, showing both Q^- (at 440 nm) and PTZ^+ (at 510 nm). Reproduced by permission of Wiley–VCH from Ref. [78].

it was clear that the charge-separated states are formed via oxidative quenching (PTZ-*Ru^{II}-Q→ PTZ-Ru^{III}-Q^-) followed by a rapid charge shift to generate the fully charge-separated state (PTZ-Ru^{III}-Q^- → PTZ^+-Ru^{II}-Q^-). This is supported by the fact that the non-oxidized triad precursors (not shown) which contain a PTZ electron donor and a methylated hydroquinone showed no quenching of emission of the Ru^{II} unit. The charge-separated states in **39** and **40** are formed in high total quantum yields ($\phi_{CS} \geq 95\%$ for **39**) with an energy of approximately 1.2 eV. The high yield was attributed to the long excited state lifetime of the dqp Ru^{II} unit as well as the fast electron transfer from the donor moiety following the initial charge separation.

6. Concluding remarks

The development of luminescent bistridentate Ru^{II} polypyridine complexes continues to be an active area of research due to their favorable structural properties. During the last years, the field has witnessed a change in the approach to achieve complexes that exhibit long lifetimes of their ^{3}MLCT states, from strategies that mainly affect the luminescent ^{3}MLCT levels to strategies where the main objective is to raise the energy of the ^{3}MC states. In this review, we have tried to summarize the results obtained so far using tridentate ligands where 6-membered chelates are obtained resulting in larger bite angles than for the related tpy ligands. Microsecond luminescent ^{3}MLCT excited state lifetimes have been obtained as a consequence of a strong ligand field, lifetimes which are even longer than those for most trisbidentate Ru^{II} polypyridine complexes. Particularly promising are the recent results on a bistridentate tetra-keto-functionalized Ru^{II} complex which combine μs lifetimes with very high quantum yield of emission, and the development of the dqp-based Ru^{II} complexes where μs lifetimes have been obtained for a large number of complexes. While the synthesis and studies of related tetra-keto-functionalized complexes awaits further advancements, the dqp Ru^{II} complexes have shown their potential to function as photosensitizer in bimolecular and intramolecular electron and/or energy transfer reactions. In particular, it has been established that directional control of photoinduced electron transfer can be achieved in multiunit assemblies based on these metal units as a result of an inherent linear arrangement. Considering their straight forward synthesis and well-behaved electrochemical and photophysical behavior, the dqp Ru^{II} family therefore will most likely be of further use in future applications.

Acknowledgements

We thank all collaborators and co-workers who have been involved in the development of novel Ru-based photosensitizers within the Swedish Consortium for Artificial Photosynthesis whose names can be found in the references. Financial support from the Swedish Research Council (VR), the Swedish Energy Agency, the Knut and Alice Wallenberg Foundation, and EU (NEST-STRP 516510 "SOLAR-H"; FP7 Energy 212508 "SOLAR-H2") is gratefully acknowledged. L.H. gratefully acknowledges a research fellow position during 2002–2007 from the Royal Swedish Academy of Science, and a generous grant from the Swedish Foundation for Strategic Research.

References

[1] M.K. Nazeeruddin, M. Grätzel, Structure & Bonding, vol. 123, Springer, Berlin/Heidelberg, 2007, 113 pp.
[2] O.S. Wenger, Coord. Chem. Rev. 253 (2009) 1439.
[3] J.H. Alstrum-Acevedo, M.K. Brennaman, T.J. Meyer, Inorg. Chem. 44 (2005) 6802.
[4] M.H.V. Huynh, D.M. Dattelbaum, T.J. Meyer, Coord. Chem. Rev. 249 (2005) 457.
[5] S. Campagna, F. Puntoriero, F. Nastasi, G. Bergamini, V. Balzani, Top. Curr. Chem. 280 (2007) 117.
[6] F. Barigelletti, L. Flamigni, Chem. Soc. Rev. 29 (2000) 1.
[7] A. Harriman, R. Ziessel, in: M.M. Haley, R.R Tykwinski (Eds.), Carbon-Rich Compounds, Wiley–VCH, Weinheim, 2006, p. 26.
[8] M.J. Cook, A.P. Lewis, G.S.G. McAuliffe, V. Skarda, A.J. Thomson, J.L. Glasper, D.J. Robbins, J. Chem. Soc., Perkin Trans. 2 (1984) 1293.
[9] M. Falkenström, O. Johansson, L. Hammarström, Inorg. Chim. Acta 360 (2007) 741.
[10] J.-P. Collin, P. Gavina, V. Heitz, J.-P. Sauvage, Eur. J. Inorg. Chem. (1998) 1.
[11] J.-P. Sauvage, J.-P. Collin, J.-C. Chambron, S. Guillerez, C. Coudret, V. Balzani, F. Barigelletti, L. De Cola, L. Flamigni, Chem. Rev. 94 (1994) 993.
[12] L. Flamigni, J.-P. Collin, J.-P. Sauvage, Acc. Chem. Res. 41 (2008) 857.
[13] J.R. Winkler, T. Netzel, C. Creutz, N. Sutin, J. Am. Chem. Soc. 109 (1987) 2381.
[14] J.-P. Collin, S. Guillerez, J.-P. Sauvage, F. Barigelletti, L. De Cola, L. Flamigni, V. Balzani, Inorg. Chem. 30 (1991) 4230.
[15] P. Lainé, F. Bedioui, E. Amouyal, V. Albin, F. Berruyer-Penaud, Chem. Eur. J. 8 (2002) 3162.
[16] O. Johansson, M. Borgström, R. Lomoth, M. Palmblad, J. Bergquist, L. Hammarström, L. Sun, B. Åkermark, Inorg. Chem. 42 (2003) 2908.
[17] J.M. Calvert, J.V. Caspar, R.A. Binstead, T.D. Westmoreland, T.J. Meyer, J. Am. Chem. Soc. 104 (1982) 6620.
[18] E.A. Medlycott, G.S. Hanan, Chem. Soc. Rev. 34 (2005) 133.
[19] E.A. Medlycott, G.S. Hanan, Coord. Chem. Rev. 250 (2006) 1763.
[20] The term "expanded ligands" are avoided in the current review as that is usually referred to ditopic ligands in which the binding sites are separated by a metal-containing unit, see *e.g.* E.C. Constable, Coord. Chem. Rev. 252 (2008) 842.
[21] A. Juris, V. Balzani, F. Barigelletti, S. Campagna, P. Belser, A. von Zelewsky, Coord. Chem. Rev. 84 (1988) 85.
[22] O.A. Borg, S.S.M.C. Godinho, M.J. Lundqvist, S. Lunell, P. Persson, J. Phys. Chem. A 112 (2008) 4470.
[23] S. Boyde, G.F. Strouse, W.A. Jones Jr., T.J. Meyer, J. Am. Chem. Soc. 112 (1990) 7395.
[24] J.A. Treadway, B. Loeb, R. Lopez, P.A. Anderson, F.R. Keene, T.J. Meyer, Inorg. Chem. 35 (1996) 2242.
[25] R. Passalacqua, F. Loiseau, S. Campagna, Y.-Q. Fang, G.S. Hanan, Angew. Chem. Int. Ed. 42 (2003) 1608.
[26] J. Wang, G.S. Hanan, F. Loiseau, S. Campagna, Chem. Commun. (2004) 2068.
[27] E.C. Constable, A.M.W. Cargill Thompson, N. Armaroli, V. Balzani, M. Maestri, Polyhedron 11 (1992) 2707.

[28] M. Maestri, N. Armaroli, V. Balzani, E.C. Constable, A.M.W. Cargill Thompson, Inorg. Chem. 34 (1995) 2759.
[29] J. Wang, Y.-Q. Fang, G.S. Hanan, F. Loiseau, S. Campagna, Inorg. Chem. 44 (2005) 5.
[30] V. Grosshenny, A. Harriman, R. Ziessel, Angew. Chem. Int. Ed. 34 (1995) 2705.
[31] Y.-Q. Fang, N.J. Taylor, G.S. Hanan, F. Loiseau, R. Passalacqua, S. Campagna, H. Nierengarten, A. Van Dorsselaer, J. Am. Chem. Soc. 124 (2002) 7912.
[32] S. Encinas, L. Flamigni, F. Barigelletti, E.C. Constable, C.E. Housecroft, E.R. Schofield, E. Figgemeier, D. Fenske, M. Neuburger, J.G. Vos, M. Zehnder, Chem. Eur. J. 8 (2002) 137.
[33] A.C. Benniston, G. Chapman, A. Harriman, C.A. Sams, Inorg. Chem. 43 (2004) 4227.
[34] Y.-Q. Fang, N.J. Taylor, F. Laverdière, G.S. Hanan, F. Loiseau, F. Nastasi, S. Campagna, H. Nierengarten, E. Leize-Wagner, A. Van Dorsselaer, Inorg. Chem. 46 (2007) 2854.
[35] J.-P. Collin, M. Beley, J.-P. Sauvage, F. Barigelletti, Inorg. Chim. Acta 186 (1991) 91.
[36] M. Beley, S. Chodorowski, J.-P. Collin, J.-P. Sauvage, L. Flamigni, F. Barigelletti, Inorg. Chem. 33 (1994) 2543.
[37] E.C. Constable, A.M.W. Cargill Thompson, J. Cherryman, T. Liddiment, Inorg. Chim. Acta 235 (1995) 165.
[38] F. Barigelletti, B. Ventura, J.-P. Collin, R. Kayhanian, P. Gaviña, J.-P. Sauvage, Eur. J. Inorg. Chem. (2000) 113.
[39] S.H. Wadman, M. Lutz, D.M. Tooke, A.L. Spek, F. Hartl, R.W.A. Havenith, G.P.M. van Klink, G. van Koten, Inorg. Chem. 48 (2009) 1887.
[40] S.H. Wadman, J.M. Kroon, K. Bakker, M. Lutz, A.L. Spek, G.P.M. van Klink, G. van Koten, Chem. Commun. (2007) 1907.
[41] M.T. Indelli, C.A. Bignozzi, F. Scandola, J.-P. Collin, Inorg. Chem. 37 (1998) 6084.
[42] M. Duati, S. Fanni, J.G. Vos, Inorg. Chem. Commun. 3 (2000) 68.
[43] M. Duati, S. Tasca, F.C. Lynch, H. Bohlen, J.G. Vos, S. Stagni, M.D. Ward, Inorg. Chem. 42 (2003) 8377.
[44] S.U. Son, K.H. Park, Y.-S. Lee, B.Y. Kim, C.H. Choi, M.S. Lah, Y.H. Jang, D.-J. Jang, Y.K. Chung, Inorg. Chem. 43 (2004) 6896.
[45] H.-F. Suen, S.W. Wilson, M. Pomerantz, J.L. Walsh, Inorg. Chem. 28 (1989) 786.
[46] R. Ziessel, V. Grosshenny, M. Hissler, C. Stroh, Inorg. Chem. 43 (2004) 4262.
[47] E.C. Constable, A.M.W. Cargill Thompson, Inorg. Chim. Acta 223 (1994) 177.
[48] Y. Jahng, R.P. Thummel, S.G. Bott, Inorg. Chem. 36 (1997) 3133.
[49] H. Wolpher, O. Johansson, M. Abrahamsson, M. Kritikos, L. Sun, B. Åkermark, Inorg. Chem. Commun. 7 (2004) 337.
[50] T. Norrby, A. Börje, L. Zhang, B. Åkermark, Acta Chem. Scand. 52 (1998) 77.
[51] M. Abrahamsson, H. Wolpher, O. Johansson, J. Larsson, M. Kritikos, L. Eriksson, P.-O. Norrby, J. Bergquist, L. Sun, B. Åkermark, L. Hammarström, Inorg. Chem. 44 (2005) 3215.
[52] M. Abrahamsson, M.J. Lundqvist, H. Wolpher, O. Johansson, L. Eriksson, J.,R.T. Bergquist, H.-C. Becker, L. Hammarström, P.O. Norrby, B. Åkermark, P. Persson, Inorg. Chem. 47 (2008) 3540.
[53] M.E. Jung, G. Piizzi, Chem. Rev. 105 (2005) 1735.
[54] O. Johansson, R. Lomoth, Chem. Commun. (2005) 1578.
[55] O. Johansson, L.O. Johannissen, R. Lomoth, Chem. Eur. J. 15 (2009) 1195.
[56] T. Bark, R.P. Thummel, Inorg. Chem. 44 (2005) 8733.
[57] F. Schramm, V. Meded, H. Fliegl, K. Fink, O. Fuhr, Z. Qu, W. Klopper, S. Finn, T.E. Keyes, M. Ruben, Inorg. Chem. 48 (2009) 5677.
[58] G. Dyker, O. Muth, Eur. J. Org. Chem. (2004) 4319.
[59] X.-D. Chen, T.C.W. Mak, Inorg. Chim. Acta 358 (2005) 1107.
[60] M. Abrahamsson, H.-C. Becker, L. Hammarström, C. Bonnefous, C. Chamchoumis, R.P. Thummel, Inorg. Chem. 46 (2007) 10354.
[61] Y.Z. Hu, M.H. Wilson, R. Zong, C. Bonnefous, D.R. McMillin, R.P. Thummel, Dalton Trans. (2005) 354.
[62] M. Abrahamsson, M. Jäger, T. Österman, L. Eriksson, P. Persson, H.-C. Becker, O. Johansson, L. Hammarström, J. Am. Chem. Soc. 128 (2006) 12616.
[63] M. Jäger, R.J. Kumar, H. Görls, J. Bergquist, O. Johansson, Inorg. Chem. 48 (2009) 3228.
[64] A.M.W. Cargill Thompson, Coord. Chem. Rev. 160 (1997) 1.
[65] R.P. Thummel, Terpyridine, Oligopyridine, and Polypyridine Ligands, vol. 1, Elsevier Ltd, 2003, p. 41.
[66] M. Heller, U.S. Schubert, Eur. J. Org. Chem. (2003) 947.
[67] J. Wang, G.S. Hanan, Synlett (2005) 1251.
[68] K.N. Campbell, J.F. Kerwin, R.A. LaForge, B.K. Campbell, J. Am. Chem. Soc. 68 (1946) 1844.
[69] M. Jäger, L. Eriksson, J. Bergquist, O. Johansson, J. Org. Chem. 72 (2007) 10227.
[70] G.A. Molander, B. Biolatto, J. Org. Chem. 68 (2003) 4302.
[71] M. Jäger, Beyond classical Ruthenium(II) polypyridyl complexes, PhD thesis, Uppsala University, Uppsala, 2009.
[72] D.A. Conlon, A. Drahus-Paone, G.-J. Ho, B. Pipik, R. Helmy, J.M. McNamara, Y.-J. Shi, J.M. Williams, D. Macdonald, D. Deschenes, M. Gallant, A. Mastracchio, B. Roy, J. Scheigetz, Org. Process Res. Dev. 10 (2006) 36.
[73] M. Jäger, O. Johansson, Unpublished work.
[74] M. Abrahamsson, M. Jäger, R.J. Kumar, T. Österman, P. Persson, H.-C. Becker, O. Johansson, L. Hammarström, J. Am. Chem. Soc. 130 (2008) 15533.
[75] J. Van Houten, R.J. Watts, J. Am. Chem. Soc. 98 (1976) 4853.
[76] M. Abrahamsson, H.-C. Becker, L. Hammarström, Work in progress.
[77] B. Durham, J.L. Walsh, C.L. Carter, T.J. Meyer, Inorg. Chem. 19 (1980) 860.
[78] R.J. Kumar, S. Karlsson, D. Streich, A. Rolandini Jensen, M. Jäger, H.-C. Becker, O. Johansson, L. Hammarström, Chem. Eur. J. (2009), doi:10.1002/chem.200902716.
[79] M. Heller, U.S. Schubert, Synlett (2002) 751.
[80] K. Lashgari, M. Kritikos, R. Norrestam, T. Norrby, Acta Cryst. C 55 (1999) 64.
[81] R.J. Watts, G.A. Crosby, J. Am. Chem. Soc. 94 (1972) 2606.